The mechanism of GroEL/GroES folding/refolding of protein substrates revisited†

Huw Jones,[a] Monika Preuss,[a] Michael Wright[a] and Andrew D. Miller*[a,b]

Received 16th December 2005, Accepted 6th February 2006
First published as an Advance Article on the web 3rd March 2006
DOI: 10.1039/b517879g

The thermodynamics and kinetics of zinc–cytochrome c (ZnCyt c) interactions with *Escherichia coli* molecular chaperone GroEL (Chaperonin 60; Cpn60) are described. Zinc(II)-porphyrhin represents a flexible fluorescent probe for thermodynamic complex formation between GroEL and ZnCyt c, as well as for stopped-flow fluorescence kinetic experiments. Data suggests that GroEL and GroEL/GroES-assisted refolding of unfolded ZnCyt c takes place by a mechanism that is quite close to the Anfinsen Cage hypothesis for molecular chaperone activity. However, even in the presence of ATP, GroEL/GroES-assisted refolding of ZnCyt c takes place at approximately half the rate of refolding of ZnCyt c alone. On the other hand, there is little evidence for refolding behaviour consistent with the Iterative Annealing hypothesis. This includes a complete lack of GroEL or GroEL/GroES-assisted enhancement of refolding rate constant k_2 associated with the unfolding of a putative misfolded state I^{H}_{NC} (Zn) on the pathway to the native state. Reviewing our data in the light of data from other laboratories, we observe that all forward rate enhancements or reductions could be accounted for in terms of thermodynamic coupling (adjusting positions of refolding equilibria) due to binding interactions between GroEL and unfolded protein substrates, driven by thermodynamic considerations. Therefore, we propose that *passive kinetic partitioning* should be considered the core mechanism of the GroEL/GroES molecular chaperone machinery, wherein the core function is to bind unfolded protein substrates leading to a blockade of aggregation pathways and to increases in molecular flux through productive folding pathway(s).

Introduction

Molecular chaperones are proteins that assist the folding of other proteins without being involved in their final folded state. Although the three dimensional structure of a given protein is specified by its sequence of amino acid residues, the kinetic process of protein folding frequently needs assistance *in vivo* as well as *in vitro*.[1] In this context, GroEL and GroES are remarkable (Fig. 1). Both proteins come from the bacterium *Escherichia coli*, but homologues are found in all cells of all organisms. Together they are able to assist the folding/refolding of many unfolded protein substrates. Literature remains at odds concerning the mechanism of GroEL/GroES assisted refolding of proteins, and discussion post-1999 is contradictory. The two extremes of the argument are represented by the *Anfinsen Cage hypothesis* and the *Iterative Annealing hypothesis*.

In the Anfinsen Cage hypothesis, protein-folding intermediates are sequestered as if at "infinite dilution" within GroEL cavities and so avoid even the remotest possibility for aggregation.[2–4] This requires that unfolded substrate proteins must fold completely within GroEL cavities, only to emerge when the native state is reached. In this hypothesis, each GroEL cavity is regarded as a passive "box of infinite dilution".[2] There is reasonable evidence against this hypothesis. For instance, the GroEL/GroES-assisted folding/refolding of large proteins (>60 kDa; too "large" for the GroEL cavities) is well established.[5,6] Also, the retention time of smaller protein folding intermediate states within GroEL cavities is ATP hydrolysis dependent, not protein dependent, hence folding intermediates as well as native state can be returned to free solution during the GroEL/GroES cycle depending upon the protein substrate involved (Fig. 1).[7,8] These folding intermediates have the option to rebind to GroEL in the next cycle with the possibility of then entering the native state.

The Iterative Annealing hypothesis highlights the unfolding of kinetically trapped, misfolded protein folding intermediates, but not the prevention of aggregation, thereby allowing for multiple possible attempts at correct folding.[9–11] The Iterative Annealing hypothesis does not require localisation within GroEL cavities but always assumes substrate protein binding to GroEL to be an active process that drives the unfolding of misfolded protein states, thereby increasing folding/refolding rates.[10] Such an active process suggests that the protein folding energy landscape is being remoulded thereby allowing for increases in rates (even catalysis) of protein folding/refolding.[3] Evidence against the Iterative Annealing hypothesis is also available.[12,13] For instance, although binding to GroEL can destabilize secondary structure,[14] this is not necessarily coordinated[12] and could equally well have more to do with the formation of minimum energy complexes

[a]*Imperial College Genetic Therapies Centre, Department of Chemistry Imperial College London, Flowers Building, Armstrong Road, Imperial College London, London, UK SW7 2AZ. E-mail: a.miller@imperial.ac.uk; Fax: +44 207 594 5803; Tel: +44 207 594 5773*
[b]*IC-Vec Ltd, Flowers Building, Armstrong Road, London, UK SW7 2AZ*
† The authors thank Mitsubishi Chemical Corporation and IC-Vec Ltd for supporting the Imperial College Genetic Therapies Centre.

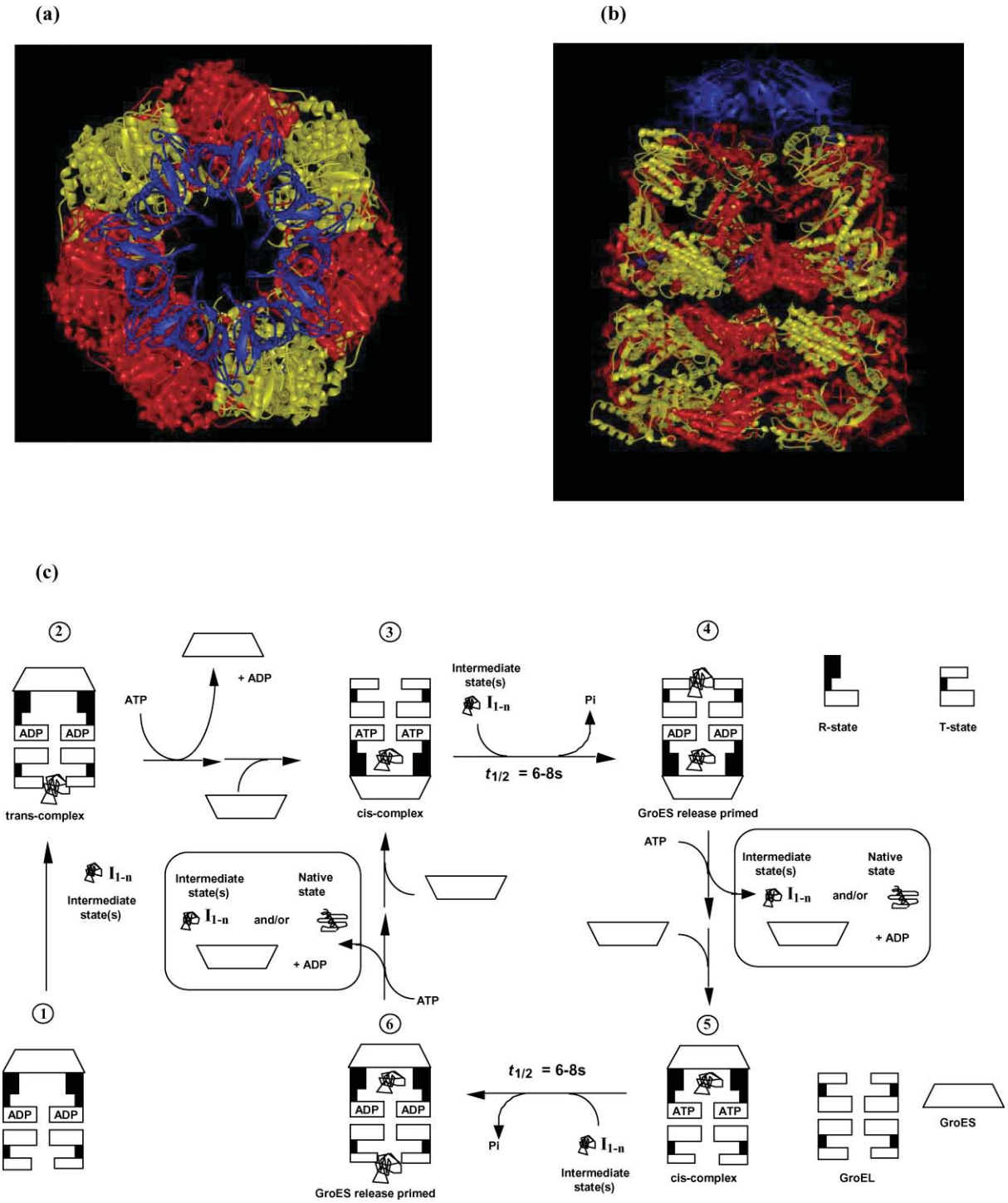

Fig. 1 Top view (a) and side view (b) of the GroEL/GroES/$(ADP)_7$ complex. GroEL is 14mer (yellow and red), each subunit 57 259 Da stacked in two rings with central cavities for protein substrate binding. GroES is 7mer (blue), each subunit 10 368 Da in a single ring of 7 subunits.[54] (c) Complete GroEL/GroES molecular chaperone machine mechanism illustrating the regular cycle of binding and release of protein substrate (in various states of unfolding).[19,43] This regular process of binding and release of protein substrate has been thought at various times to have catalytic effects on protein folding or else provide a means for the folding of substrate proteins at "infinite dilution" in the GroEL central cavities. The T-state and R-state nomenclature refer to the conformations of individual GroEL subunits in the homo-oligomeric structure. The T-state has a high affinity for substrate protein and the R-state a low affinity (the affinity for ATP is reversed). The term $\mathbf{I}_{1-n}$ refers to discrete substrate protein folding intermediates, **I**, of between **1** and ***n*** in number.

between substrate protein folding intermediates and GroEL, than a systematic and regular process of controlled unfolding through binding.[15] An Iterative Annealing mechanism should also be expected to ensure a 100% yield of folding/refolding to the native state in the absence of aggregation effects, but this is not always the case[15–17] owing to the impact of the extrinsic environment (buffer concentration, ionic strength, pH, temperature) on protein folding/refolding yields, something over which GroEL appears to have little control.[18,19]

The usual way to minimise the significance of model protein folding/unfolding data is to suggest that the substrate proteins used are "not-authentic", thereby invalidating most of the available mechanistic data concerning GroEL, including all previously published stopped-flow kinetics experiments. However, the concept that there is somehow a "pure" GroEL/GroES mechanism applicable to "real substrates" seems too extreme.[20] The wide range of model studies with different GroEL/GroES-assisted folding/refolding of model protein substrates should not be dismissed so lightly since they demonstrate how adaptive the GroEL/GroES-molecular chaperone machine can be to "meeting the needs" of individual unfolded substrate proteins in their quest for efficient, high yielding folding/refolding to the native state.[20,21] In our case, we originally considered that since GroEL and GroES share high levels of sequence identity and similarity with mammalian Hsp60 and Hsp10 respectively, then protein substrates for the Hsp60/Hsp10 machinery might reasonably be expected to be appropriate substrates for the GroEL/GroES molecular machinery as well. Accordingly, since the Hsp60/Hsp10 machinery is involved in protein import into the matrix of mammalian cell mitochondria, we surmised that mitochondrial proteins/enzymes should be appropriate analogue substrates for the GroEL/GroES-molecular machinery. This analysis led to the original selection of commercially available porcine mitochondrial malate dehydrogenase (mMDH).[18,19,22,23] In the experiments described here, equine heart cytochrome c was selected as an alternative model unfolded protein substrate for the GroEL/GroES molecular chaperone machine on the basis that this is a well characterised, small, single domain protein that folds/refolds in a known manner over an unusually long time-scale (several seconds),[15] making this protein an almost ideal substrate for spectroscopic and stopped-flow kinetic refolding studies. It is our contention that data obtained with these model unfolded protein substrates should be regarded as both meaningful and useful, to be interpreted alongside data obtained from other diverse model protein folding/refolding systems.

Data acquired from these two assays actually suggested an alternative mechanistic hypothesis, namely passive kinetic partitioning (Fig. 2). According to this mechanism, the primary role of GroEL is to bind, isolate and then release protein folding intermediates (**U** to $\mathbf{I_2}$) otherwise vulnerable to bi-/multimolecular *n*th-order aggregation processes (where $n > 2$), in a controlled and cyclical fashion so as to suppress their free, solution concentrations below a critical threshold for aggregation. In so doing, protein folding intermediates are encouraged to partition kinetically along the unimolecular pathway(s) to correct folded protein, **N**, in preference to being trapped in aggregated states [$(\mathbf{I_1})_m$ and $(\mathbf{I_2})_m$]. Essentially, the yield of correct folded protein can be maximized by a passive kinetic partitioning mechanism without requiring catalysis of the productive folding pathway(s)

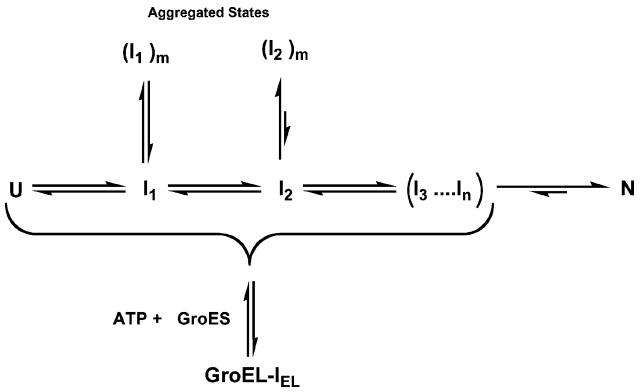

Fig. 2 Passive kinetic partitioning mechanism of the GroEL/GroES molecular chaperone machine. This mechanism assumes that protein folding is initiated at an unfolded state, **U**, which folds through a succession of intermediate states $\mathbf{I_1}$, $\mathbf{I_2}$, $(\mathbf{I_3}\cdots\mathbf{I_n})$ before reaching the native state, **N**. States $\mathbf{I_1}$ and $\mathbf{I_2}$ are considered arbitrarily to be unstable to aggregation, forming aggregated states $(\mathbf{I_1})_m$ and $(\mathbf{I_2})_m$ through interaction of their exposed hydrophobic surfaces. GroEL is potentially able to bind to all vulnerable protein folding intermediate states, except **N**, forming a GroEL-bound state GroEL-I_{EL}. The nature of this state is a function of the requirement to optimise the free energy of association between GroEL and the given unfolded protein state under the given set of binding conditions. The binding interaction with GroEL is reversed in a controlled manner with the assistance of first adenosine 5′-triphosphate (ATP) and then GroES binding, after which the protein substrate is retained by the GroEL intra-cavity until ATP hydrolysis is complete ($t_{1/2}$ 6–8 s). Thereafter, the protein substrate may be released into free solution ready to rebind again if necessary (see Fig. 1). As a result of this cyclical binding and controlled release into a GroEL cavity and then free solution, steady state concentrations of **U**, $\mathbf{I_1}$, $\mathbf{I_2}$ and $(\mathbf{I_3}\cdots\mathbf{I_n})$ are maintained below the critical threshold for aggregation so that these states are free to partition kinetically to **N**.[15]

or any other significant intervention. That is unless the yield is otherwise reduced by unimolecular protein misfolding resulting from incorrect intramolecular interactions formed in response to the extrinsic folding conditions. In this latter case, such misfolded proteins could in principle rebind/bind to GroEL but would only be rescued if the molecular chaperone were able to muster sufficient binding energy to reverse those incorrect intramolecular interactions by means of unfolding mechanisms.[14,24] According to this mechanism, GroEL is otherwise unlikely to have much capacity to influence the role of the extrinsic folding conditions in protein folding.

The utility of the passive kinetic partitioning mechanism is that it can accommodate features of both of the two main mechanistic hypotheses in such a way as to make sense of the negative evidence against both. For instance, the binding of large and small protein folding intermediates and their subsequent release into free solution (in contradiction to the Anfinsen Cage mechanism), and the fact that GroEL/GroES assisted folding/refolding of proteins rarely results in a 100% recovery of correct folded protein in assay systems[15] (in contradiction to Iterative Annealing), makes sense with the passive kinetic partitioning mechanism. The Iterative Annealing mechanism also suggests the likelihood of rate enhancements in protein folding/refolding as a consequence of GroEL/GroES assistance. By contrast, an important consequence of the passive kinetic partitioning mechanism is to diminish the

likelihood that the GroEL/GroES machinery is able to enhance rates or catalyse protein folding/unfolding as a rule. Instead, the mechanism suggests that protein folding/refolding is assisted primarily by increasing molecular flux through productive folding pathways, employing cyclical binding and release to retard the kinetic partition of molecular flux though irreversible, higher-order aggregation pathways. Previously, we showed very clearly that mMDH will refold to give a 100% yield of the native state in the presence of GroEL and GroES, by increasing molecular flux through the correct folding pathway, and without changing first and second order rate constants for refolding.[22,23] Here we report additional information concerning GroEL/GroES assisted folding/refolding of proteins using a novel zinc form of equine heart cytochrome c, known as zinc-cytochrome c (ZnCyt c). Data from thermodynamic and stopped-flow fluorescence kinetic studies are reported that agree closely with conclusions obtained with the mMDH model.

Results and discussion

Various thermodynamic binding and kinetic studies were performed using specially prepared ZnCyt c in place of equine cytochrome c. ZnCyt c has an essentially identical three-dimensional structure to cytochrome c (Scheme 1),[25,26] and hence binds to cytochrome c oxidase in an equivalent manner to cytochrome c.[27] There are three main differences. Firstly, ZnCyt c exhibits intrinsic Zn(II)porphyrin fluorescence (I_{max} 588 nm), whereas cytochrome c exhibits little intrinsic heme fluorescence, and both I_{max} and the fluorescence quantum yield are sensitive to protein conformation. Secondly, ZnCyt c is structurally a little less stable than cytochrome c.[28] Thirdly, Zn(II) unlike Fe(II) or Fe(III) is not redox active owing to complete 3d orbital occupancy.

For the first two reasons, we considered that ZnCyt c would be a more useful tool (*cf.* to cytochrome c) to evaluate the effects of the GroEL/GroES molecular chaperone machine on protein folding/refolding. Changes in intrinsic Zn(II)porphyrin fluorescence offer a unique, sensitive probe for extent of folding as a function of time at concentrations of ZnCyt c well below the potential threshold for aggregation. Also, the lower intrinsic stability suggested that GroEL-protein interactions would be stronger than those observed with cytochrome c previously,[15] and hence lead to more pronounced and realistic molecular chaperone effects. Hence, ZnCyt c was prepared from cytochrome c as described (see Materials and Methods) and thermodynamic binding studies were carried out initially to verify comparable behaviour with cytochrome c. Thereafter a series of stopped-flow kinetics studies were performed.

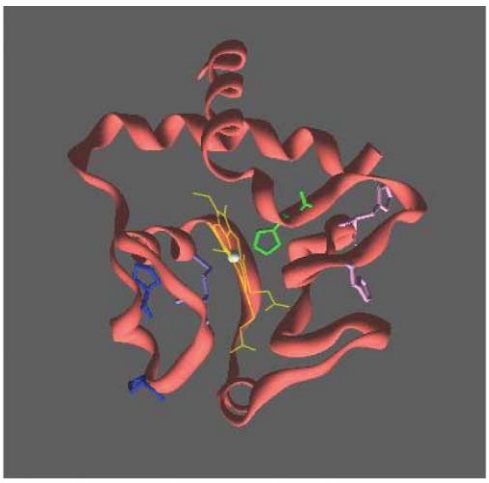

Scheme 1 Refolding of cytochrome c and ZnCyt c. (*Top*) Ribbon display structure (side view) of the X-ray crystal structure of horse heart cytochrome c (RCSB Protein Data Bank: 1 hrc).[55] The ribbon represents the α-carbon backbone. Illustrated amino acid residues are: histidine residue 18 (H18) (green) and histidine residues (H26 and H33) (light purple): methionine residue (M80) (cyan): proline residues (P71 and P76) (blue). The covalently attached heme group of cytochrome c may be seen at the centre of the structure, sideways on (yellow) with the central iron atom illustrated (white sphere). (*Middle*) Cytochrome c folding pathway adapted from Colón *et al.*[32] **U** corresponds to unfolded states and **I** to intermediate states. **N*** is a native-like state of cytochrome c with the M80 ligand displaced and $\mathbf{N^M}$ the final biologically active native state of cytochrome c. See text for details. (*Bottom*) Equivalent folding pathway deduced for ZnCyt c.

Thermodynamic interactions with GroEL

As with cytochrome c,[15] both native and 8 M urea-unfolded ZnCyt c were able to form complexes with GroEL (in 25 mM Tris-acetate, pH 7.4) that were stable enough to be isolated by gel filtration (Sephadex S-300) free of unbound ZnCyt c protein (results not shown). UV–Visible spectra of GroEL-bound and free ZnCyt c were recorded and absorption maxima data compiled (Table 1). The spectral properties of the complex formed between unfolded ZnCyt c protein and GroEL were found to lie between the properties of unfolded and native ZnCyt c. Therefore, GroEL-bound unfolded ZnCyt c appears to be trapped in a state closer in character to the ZnCyt c native state than the unfolded state. In a similar way, the spectral properties of the complex formed between native ZnCyt c protein and GroEL were found to lie even closer to the properties of native ZnCyt c. Therefore, GroEL-bound native ZnCyt c appears to be trapped in an almost native-like state. These properties are essentially very similar to those reported previously for cytochrome c.[15]

Table 1 Summary of UV–visible fluorescence and absorption data obtained from unfolded ZnCyt c, native ZnCyt c, GroEL-bound unfolded ZnCyt c and GroEL-bound native ZnCyt c. All data were recorded in 25 mM Tris-acetate, pH 7.4, at 22 °C in a 1 cm pathlength cell with slit-widths of 5 nm (excitation and emission) for fluorescence. [ZnCyt c] was normalized to 3 μM

ZnCyt c state	Soret band absorption λ_{max}/nm	Soret band fluorescence I_{max}/nm (excitation λ_{max}/nm)	α/β bands
Native	423	588.0 (412)	549 585
GroEL-bound native	424	587.8 (411)	550 583
GroEL-bound unfolded	422	587.4 (408)	550 583
Unfolded	421	582.8 (407)	547 582

Fluorescence titration binding experiments were then performed in which a fixed concentration of either native or 8 M urea-unfolded ZnCyt c (1 μM) was titrated with GroEL (0–1 μM) at 22 °C over a period of 30 min (Fig. 3), and the change in intensity of I_{588}, ΔI_{588}, plotted as a function of GroEL concentration. The apparent association constants, $K_{d\,app}$, were then determined. These values of $K_{d\,app}$ were determined given a number of assumptions. These were;

1) each GroEL binding site has equal affinity for unfolded ZnCyt c,

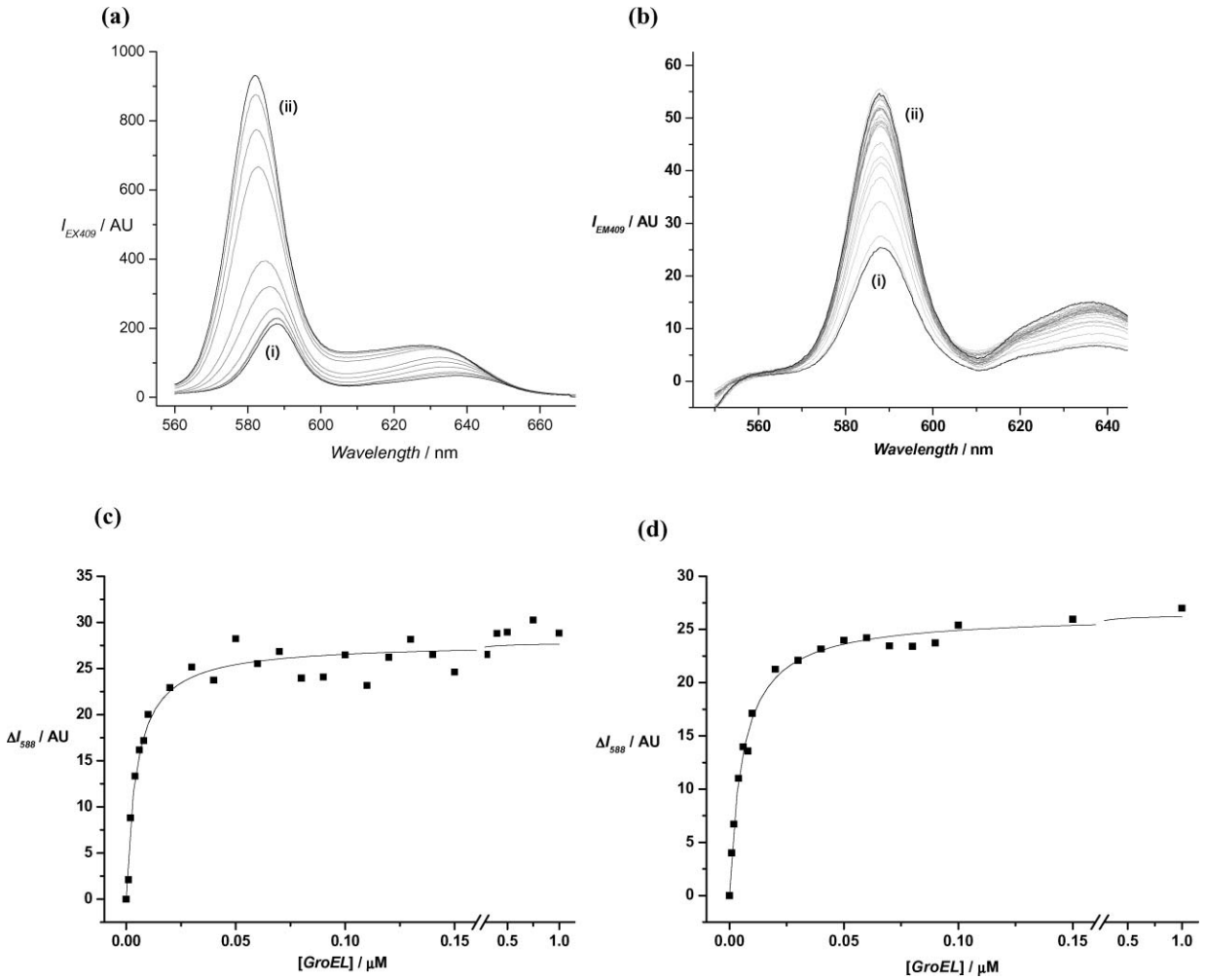

Fig. 3 ZnCyt c fluorescence spectra. (a) Fluorescence unfolding titration experiment showing porphyrin fluorescence emission spectra of ZnCyt c (7 μM) in 25 mM Tris-acetate, pH 7.4, with 2 mM β-ME, in the presence of increasing concentrations of urea from 0 M (i) up to 9 M (ii). (b) Porphyrin fluorescence emission spectra of unfolded ZnCyt c (1 μM final concentration) added to 25 mM Tris-acetate, pH 7.4, with 2 mM β-ME in the presence of increasing concentrations of GroEL from (0–1 μM final homo-oligomer concentration) where (i) is spectrum without GroEL and (ii) is spectrum with 1 μM GroEL. (c) Fluorescence binding titration isotherm for the binding of unfolded ZnCyt c to GroEL obtained by plotting fluorescence intensity change at 588 nm, ΔI_{588}, against GroEL homo-oligomer concentration. (d) Fluorescence binding titration isotherm for the binding of native ZnCyt c to GroEL obtained by plotting fluorescence intensity change at 588 nm, ΔI_{588}, against GroEL homo-oligomer concentration. Data from (c) and (d) was fitted to a one site-binding model to obtain dissociation constant data. Fluorescent excitation was at 423 nm throughout. The temperature was at 22 °C. For other parameters see Table 1.

2) each unfolded ZnCyt c molecule interacts with only one potential GroEL binding site and therefore is unable to interact with any other GroEL molecule at the same time,

3) binding sites are spectroscopically indistinguishable from each other and the binding of each ZnCyt c results in an equal change in fluorescence.

$K_{d\,app}$ values were found to be 1.2 ± 0.3 nM or 0.8 ± 0.4 nM for native or 8 M urea-unfolded ZnCyt c respectively. The tight binding of native ZnCyt c (Fig. 3) probably reflects the capacity of GroEL to interact with a small equilibrium pool of native ZnCyt c possessing transiently unfolded regions that GroEL is able to bind to, thus shifting the ZnCyt c conformational equilibrium towards further unfolding and further binding to GroEL according to the law of mass action. Another single domain protein dihydrofolate reductase (DHFR) has been shown to behave similarly.[29] The binding of unfolded ZnCyt c reflects kinetic trapping of a variety of folding intermediate states converging to a minimum energy bound state. Other studies have shown that each GroEL may bind up to five cytochrome c molecules.[15] Therefore, assuming this to be the case, we can use the following eqn (1):

$$\kappa_d = nK_{d,\,app} \quad (1)$$

to determine microscopic dissociation constant values, κ_d, where n is the number of putative binding sites (in this case 5). Hence the κ_d value for unfolded ZnCyt c is 3.9 nM and the value for native ZnCyt c is 5.8 nM. These figures compare very well with previous $K_{d\,app}$ and κ_d values,[24] and if anything, suggest that ZnCyt c binds to GroEL with an affinity as great if not greater than most other proteins examined recently.

Finally, ZnCyt c aggregation studies were performed using light scattering intensity at 500 nm, I_{500}, as a means to detect the formation of protein aggregates in solution. This technique was used previously to demonstrate that the presence of GroEL can suppress the aggregation of unfolded citrate synthase (CS) by binding and sequestration of vulnerable CS protein folding intermediates.[17] Unfolded ZnCyt c was found not to undergo visible aggregation below 10 μM. Above this concentration aggregation was observed (Fig. 4), but an equimolar concentration of GroEL was sufficient to reduce this aggregation substantially, presumably through the binding and sequestration of vulnerable ZnCyt c protein folding intermediates in a comparable manner to CS. At concentrations of below 10 μM, unfolded ZnCyt c in the process of folding may be assumed to be at minimal risk of aggregation (under these experimental conditions). Therefore, 10 μM represents the upper limit for the concentration of unfolded ZnCyt c in stopped-flow kinetic studies that is required to avoid analytical complications from aggregation processes and also that is required in order to test one of the key predictions of the Iterative Annealing hypothesis, that assisted folding through iterative annealing should result in enhancements in rates of refolding at concentrations below the aggregation threshold.

Stopped-flow kinetic analyses; cytochrome c *versus* ZnCyt c

The refolding behaviour of ZnCyt c has not been substantially characterised, therefore our first objective was to verify whether or not the refolding characteristics of ZnCyt c were similar to those of cytochrome c using stopped-flow kinetic analyses. The refolding of cytochrome c has been studied intensively.[30] For such a small, single domain protein, the rate of refolding is surprisingly slow compared with other equivalent proteins (<20 kDa) that usually refold spontaneously in a matter of a few milliseconds. By contrast, unfolded cytochrome c takes approximately 10 s to reach its native state at 22 °C and neutral pH. This is an ideal time-scale to study GroEL/GroES-assisted refolding by means of stopped-flow kinetics experiments since this time-scale is almost equivalent to the half-life (6–8 s) of substrate protein sequestration within GroEL cavities.[31] Hence, if ZnCyt c were similar to cytochrome c then refolding ZnCyt c might be expected to be an almost ideal probe to study the kinetic impact of cavity sequestration (Fig. 1). Furthermore, refolding ZnCyt c might be expected to form a transient misfolded state at neutral pH, that could act as an ideal probe to study whether or not binding to GroEL leads to assisted unfolding of the misfolded state with concomitant increases in refolding rates.

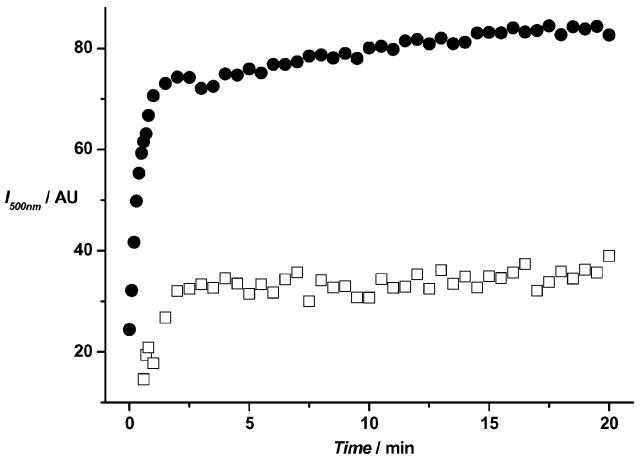

Fig. 4 Aggregation of unfolded ZnCyt c observed by light scattering. 8 M Urea-unfolded ZnCyt c (15 μM final concentration) is dispersed in 25 mM Tris-acetate, pH 7.4, with 2 mM β-ME, at 22 °C, in the absence (●) or presence of GroEL (□) (15 μM final homo-oligomer concentration). Scattered light intensity, I_{500}, was observed over time.

The unusually slow refolding behaviour of cytochrome c is down to the presence of the heme group. In the native state of cytochrome c, the heme iron atom is axially coordinated by histidine 18 (H18) and methionine 80 (M80). At neutral pH, the predominant unfolded state of cytochrome c is known as $\mathbf{U^H}$. In this state, the heme iron remains coordinated by H18 but the M80 ligand found in the native state is replaced either by histidine 26 (H26) or histidine (H33) (Scheme 1).[32] Of these latter two residues, H33 is used most frequently.[33] The first event in refolding at low denaturant concentrations (<1.5 M guanidinium chloride [Gu–HCl]), is the rapid formation (≈1 ms) of a compact intermediate, $\mathbf{I^H_C}$ (Scheme 1). Refolding then continues through a partially folded intermediate, $\mathbf{I^H_{NC}}$, which is stabilised through the interaction of the main N- and C-terminal α-helices.[34] In this transient misfolded state the heme iron still remains coordinated by either H26 or H33, thereby preventing the formation of stable secondary and tertiary structures in other regions of the protein. In order for the native state to form, the non-native histidine residue must dissociate to generate a five-coordinate molten globule intermediate $\mathbf{I^*_{NC}}$. This dissociation step is one of the key rate limiting steps in cytochrome c refolding at neutral pH. The refolding process is then completed by slow *cis* to *trans* isomerisation of proline 71 (P71) and

Table 2 Summary of stopped-flow fluorescence kinetic data obtained from the refolding of 8 M urea unfolded cytochrome c (10 μM) monitored at 22 °C in 25 mM Tris-acetate buffer, pH 7.4, by intrinsic tryptophan fluorescence (excitation 280 nm; emission >320 nm), compared with data obtained from 8 M urea unfolded ZnCyt c refolding under the same conditions but monitored by both intrinsic tryptophan (excitation 280 nm; emission >320 nm) and Zn(II)porphyrin fluorescence (excitation 409 nm; emission >455 nm). [ZnCyt c] was 10 μM and 2 μM respectively for the two ZnCyt c refolding experiments as described in the text

Protein	Fluorophore	k_1/s^{-1}	Amp1 (%)	k_2/s^{-1}	Amp2 (%)	k_3/s^{-1}	Amp3 (%)
Cytochrome c	Trp	52.1 ± 1.6	37.9 ± 0.7	2.9 ± 0.4	44.8 ± 2.2	0.34 ± 0.04	17.3 ± 1.9
ZnCyt c	Trp	18.1 ± 2.6	46.7 ± 1.1	3.0 ± 1.0	26.9 ± 2.6	0.17 ± 0.05	26.4 ± 2.2
ZnCyt c	Porphyrin	22.3 ± 4.8	46.1 ± 3.2	5.8 ± 1.7	29.0 ± 4.2	0.10 ± 0.04	24.9 ± 4.2

proline 76 (P76) to give a five-coordinate state **N*** that rapidly assembles into the native state, $\mathbf{N^M}$, wherein methionine 80 (M80) coordinates the central heme iron atom (Scheme 1).[32,35,36]

This mechanism in effective kinetic terms represents a three-state refolding process in which dilution from the denaturant initially involves a fast phase (k_1) of refolding culminating in the formation of a transient misfolded state $\mathbf{I^H_{NC}}$. Thereafter, formation of the five-coordinate molten globule state $\mathbf{I^*_{NC}}$ takes place from the misfolded state in a slow phase (k_2) of refolding. Finally, *cis* to *trans* prolyl isomerisation takes place during a second slow phase (k_3) of refolding to give the five-coordinate state **N***. By means of a sequence of stopped-flow fluorescence kinetic experiments, we obtained a complete set of kinetic data by monitoring the refolding of both 8 M urea unfolded-cytochrome c and 8 M urea unfolded-ZnCyt c post dilution into 25 mM Tris-acetate buffer, pH 7.4 (Table 2). Cytochrome c refolding was monitored by means of intrinsic tryptophan [W59] fluorescence, ZnCyt c refolding by means of both intrinsic tryptophan and Zn(II)porphyrin fluorescence. The results clearly demonstrate that unfolded-ZnCyt c refolds in a comparable manner to cytochrome c (see Scheme 1), and so is a worthy surrogate after all, even if k_1 is slower then the cytochrome c equivalent rates.

A reasonable explanation for this rate constant difference is that Zn(II) coordination of histidine residues H26 or H33 is less avid than Fe(II)/Fe(III) coordination hence the transition state leading to this putative transient, misfolded state $\mathbf{I^H_{NC}}$ (Zn) of ZnCyt c should be of a higher energy than that of cytochrome c and hence forms less readily. We note in consideration of the kinetic similarity of cytochrome c and ZnCyt c refolding, that the observed thermodynamic complex formed between unfolded ZnCyt c and GroEL may be regarded as a primary combination of GroEL with the transient, misfolded state $\mathbf{I^H_{NC}}$ (Zn) and the five-coordinate molten globule-state $\mathbf{I^*_{NC}}$ (Zn). In a similar way, the observed thermodynamic complex formed between native ZnCyt c and GroEL may be represented as a primary combination of GroEL with the putative five-coordinate state **N*** (Zn). Such interpretations would be consistent with the observed spectroscopic data (Fig. 3) and would also be consistent with our previous work concerning GroEL-cytochrome c complexes.[15]

Stopped-flow kinetic analyses with GroEL and GroES

Representative stopped-flow fluorescence data is shown following the high speed mixing of 8 M urea-unfolded ZnCyt c (2 μM final concentration) and various concentrations of GroEL (0–4 μM final concentration of oligomer) (Fig. 5). Calculated values of k_1, k_2 and k_3 are shown as a function of increasing GroEL concentration, as well as the change in signal amplitude as a function of increasing GroEL concentration (Fig. 5), all recorded at 22 °C in 25 mM Tris-acetate buffer, pH 7.6. Rates of k_1 and k_2 decline markedly with increasing GroEL. k_3 is essentially unaffected. In other words, GroEL is actively retarding k_1, the rate constant for formation of the putative misfolded state $\mathbf{I^H_{NC}}$ (Zn), and also k_2 the rate constant for unfolding the putative misfolded state $\mathbf{I^H_{NC}}$ (Zn) into the putative five-coordinate molten globule-state $\mathbf{I^*_{NC}}$ (Zn). Since aggregation of ZnCyt c occurs at >10 μM (Fig. 4), then GroEL alone is clearly not promoting rate enhancements through unfolding misfolded ZnCyt c under conditions where there is no aggregation. Such an observation runs completely counter to the Iterative Annealing hypothesis. GroEL made no impact on the k_3 rate constant for *cis* to *trans* prolyl isomerisation, but then GroEL has never been noted to possess a *cis* to *trans* isomerisation role, so this result is consistent with known GroEL behaviour.

Another interesting point to note is that fluorescence signal amplitude was observed to increase when GroEL was combined with unfolded ZnCyt c, an effect that reached a plateau from 2 μM concentration upwards (Fig. 5). This result can be explained with reference to an increase in Zn(II)porphyrin fluorescence quantum yield following thermodynamic complex formation with GroEL (Fig. 3). When equimolar concentrations of GroEL and unfolded ZnCyt c are combined by stopped-flow mixing then all the ZnCyt c must remain bound to GroEL at the conclusion of the mixing. Given the observed rate data indicative of substantial perturbations in k_1 and k_2 but not in k_3, this complex presumably involves primarily the $\mathbf{I^*_{NC}}$ (Zn) state in GroEL-bound equilibrium with the putative five-coordinate state **N*** (Zn) and the transient misfolded $\mathbf{I^H_{NC}}$ (Zn) state. Our kinetic observations here and previous thermodynamic observations concerning complex formation (see above) appear to be in good agreement.

There is another important point to note however, namely that the values of k_1 and k_2 were finite throughout and did not reduce to zero as the concentrations of GroEL and unfolded ZnCyt c approached equimolar. The retarding effect of GroEL on the first kinetic constant rate k_1 [correlating with the formation of $\mathbf{I^H_{NC}}$ (Zn)], suggests that the binding between protein and GroEL is rapid and close to diffusion control. Furthermore, suppression of the second kinetic constant k_2 [correlating with the formation of $\mathbf{I^*_{NC}}$ (Zn)] is consistent with further "on-chaperone refolding". If refolding of unfolded ZnCyt c was taking place off-chaperone then values of k_1 and k_2 should approach zero at high GroEL concentrations owing to inhibition of refolding as a result of complete sequestration of unfolded ZnCyt c. Similar results with similar conclusions were obtained when the refolding behaviours of either unfolded barnase or staphylococcal nuclease (SNase) were studied using

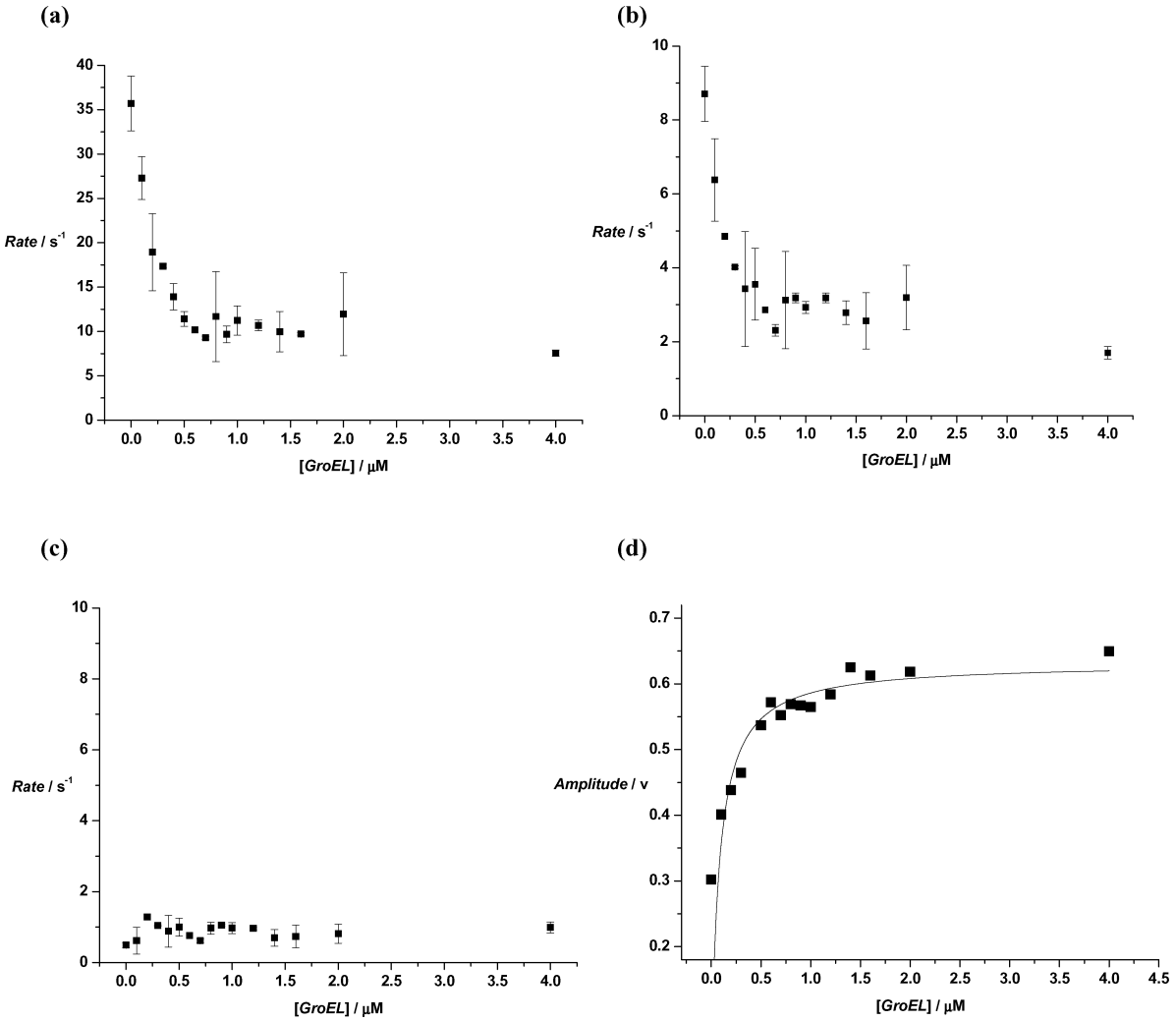

Fig. 5 Effect of GroEL on the rate of refolding of unfolded ZnCyt c determined by stopped-flow fluorescence kinetic experiments. 8 M Urea unfolded ZnCyt c (2 μM final concentration) and various concentrations of GroEL (0–4 μM final homo-oligomer concentration) were rapidly combined in 25 mM Tris-acetate, pH 7.4, with 2 mM β-ME, at 22 °C. Fluorescence changes observed with time were used to calculate variations in rate parameters as a function of GroEL homo-oligomer concentration. (a) Variation of k_1. (b) Variation of k_2. (c) Variation of k_3. (d) Variation of total amplitude.

stopped-flow fluorescence in the presence of GroEL by the research groups of Fersht and Kuwajima respectively.[37–39] By contrast, when the refolding of α-lactalbumin (α-LA) was studied by stopped-flow fluorescence in the presence of GroEL, then the slow phase of refolding was found to be retarded by GroEL to zero.[40–42] Accordingly, Kuwajima and colleagues concluded that unlike barnase and SNase, α-LA refolding on-chaperone was negligible and that "off-chaperone refolding" was in fact taking place. The difference was explained by variations in binding strength to GroEL. $K_{\mathrm{d\,app}}$ values of unfolded barnase or SNase were estimated in the nM-range and the $K_{\mathrm{d\,app}}$ value of unfolded α-LA was estimated in the μM-range. The implication is that binding in the nM-range is necessary to achieve on-chaperone folding, and that much weaker binding in the μM-range promotes off-chaperone folding by default. Consistent with this argument is the fact that the values of $K_{\mathrm{d\,app}}$ for unfolded ZnCyt c are in the nM-range, and unfolded ZnCyt c also appears to fold "on-chaperone" according to kinetic arguments, in common with unfolded barnase or SNase. However, although observed "on-chaperone refolding" appears to be associated with certain kinetic constants and steps of partial refolding, this observed process could just as well be a process of structural accommodation between GroEL and unfolded protein substrate required to minimize complex free energy and optimise binding affinity.[15] Given this scenario, unfolded α-LA could be said to have weaker capacity for structural accommodation than unfolded barnase, SNase and ZnCyt c, and therefore is able to bind less effectively to GroEL than the other three proteins by three orders of magnitude. The key point is that "on-chaperone refolding" as well as "off-chaperone refolding" could be seen as being driven fundamentally by thermodynamic considerations.

Representative stopped-flow fluorescence data is also shown following the high speed mixing of 8 M urea-unfolded ZnCyt c (2 μM final concentration) and ADP-GroEL, ATP-GroEL and ATP-GroEL/GroES together with a number of other control combinations (Fig. 6). The illustrated data shows the saturating rate constant values and total amplitudes measured with equimolar GroEL (2 μM final concentration) and equimolar GroES (2 μM

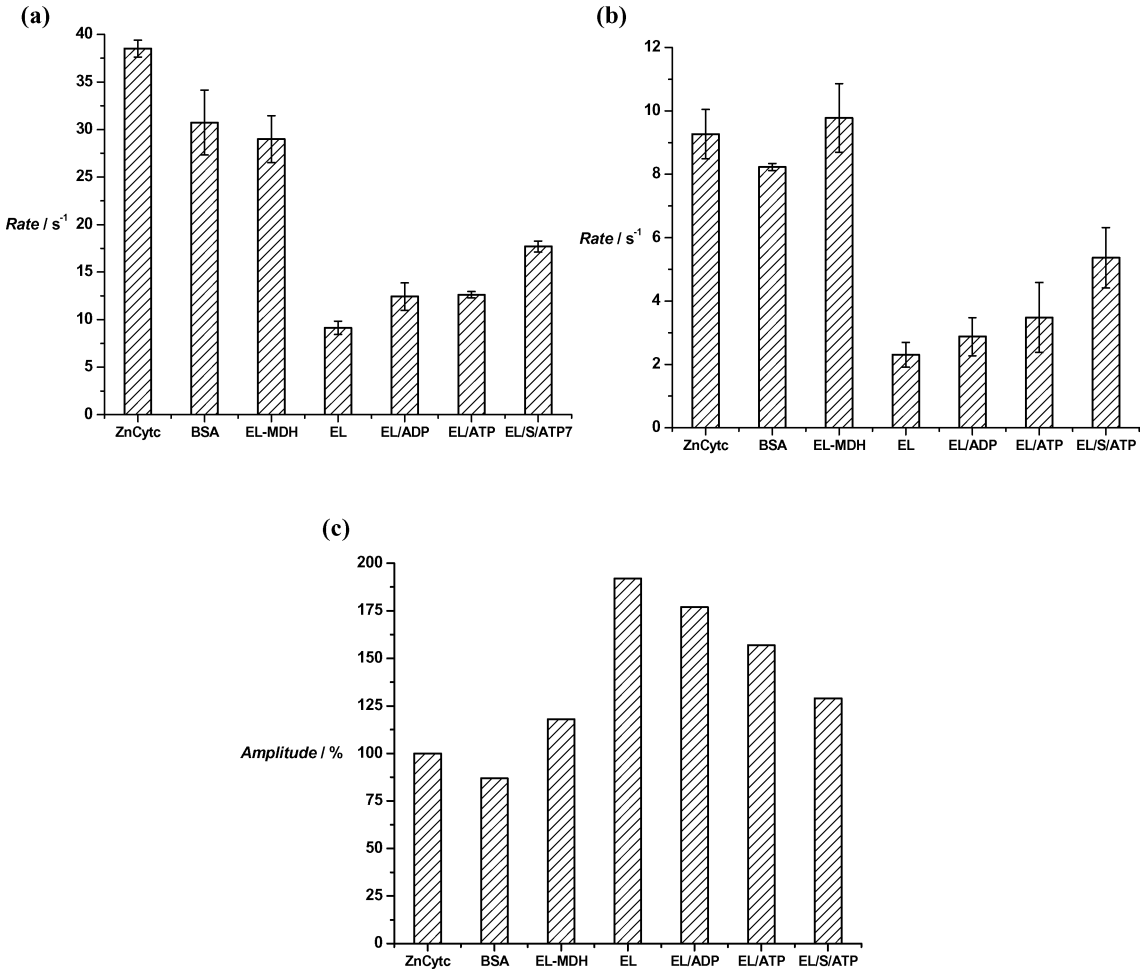

Fig. 6 Maximal effects on the kinetics of refolding of unfolded ZnCyt c as determined by stopped-flow fluorescence kinetic experiments. 8 M Urea unfolded ZnCyt c (2 μM final concentration) and various additives as indicated were rapidly combined in 25 mM Tris-acetate, pH 7.4, with 2 mM β-ME, at 22 °C, and then fluorescence changes were observed with time and used to calculate maximal rate parameters as a function of the presence of different additives. (a) Variation of k_1. (b) Variation of k_2. (c) Variation of total amplitude. Additives were either absent (ZnCyt c) or were respectively GroEL (EL) (2 μM final homo-oligomer final concentration), GroES (S) (2 μM final homo-oligomer final concentration), ADP or ATP (each 1 mM final concentration) with KCl and $MgCl_2$ (each 10 mM final concentration), bovine serum albumin (BSA) (2 μM final concentration), or 8 M Urea unfolded malate dehydrogenase (MDH) (2 μM final concentration). These were used with unfolded ZnCyt c in the combinations indicated on the Figure.

final concentration when required), where initial ADP or ATP concentrations were 1 mM with 10 mM KCl and 10 mM $MgCl_2$ to promote ATP hydrolysis (where appropriate). The data trends are interesting. In all cases, saturating k_1 and k_2 values were suppressed when unfolded ZnCyt c was refolded in the presence of different main GroEL-species (unless GroEL was preblocked with mMDH to prevent ZnCyt c binding at all). However, both values of k_1 and k_2 were seen to increase according to the main GroEL-species involved in the order GroEL < GroEL-ADP < GroEL-ATP < GroEL/GroES-ATP. By contrast, saturating fluorescence signal amplitude values were found to decrease in the order GroEL > GroEL-ADP > GroEL-ATP > GroEL/GroES-ATP. There are simple explanations for these effects in terms of the known binding affinities of the various GroEL species for unfolded protein substrates that also decease in the order GroEL > GroEL-ADP > GroEL-ATP > GroEL/GroES-ATP.[42,43] Firstly, since k_1 and k_2 rate constants appear to increase as the substrate affinities of each main GroEL-species decline, then refolding rates clearly increase as the strengths of interaction of substrate protein with each respective main GroEL-species decrease. Such effects have been seen previously with barnase[38] and especially with α-LA,[42] and interpreted in the same way. Secondly, since saturating fluorescence signal amplitude values appear to decrease as the affinities of each main GroEL-species decrease, then the proportion of ZnCyt c remaining complexed to GroEL at the end of each mixing experiment must decrease as the strength of interaction with each respective main GroEL-species decreases.

Experiments involving the combination of GroEL/GroES-ATP with unfolded ZnCyt c are closest to stopped-flow observations on the complete GroEL/GroES molecular chaperone machine. Therefore, these data are very important. In this case, k_1 and k_2 rate constants were approximately 50% lower than values obtained from the refolding of ZnCyt c alone, and the fluorescence signal amplitude was only approximately 20% higher. In other words, under conditions where there is no ZnCyt c aggregation there is a general kinetic similarity between GroEL/GroES-ATP assisted

refolding of unfolded ZnCyt c, and the refolding of unfolded ZnCyt c alone. Such an observation aligns quite closely with the Anfinsen Cage hypothesis, but not precisely since rate constants are still partially suppressed (Fig. 6). On the basis of our data with ZnCyt c, we would favour a mechanism for GroEL/GroES-assisted refolding/folding of ZnCyt c that is aligned with the Anfinsen Cage hypothesis. Our data does not appear to align with the Iterative Annealing hypothesis at all. There is a complete lack of enhancement of forward rate constants especially of k_2 that is associated with the unfolding of a putative misfolded state $\mathbf{I}^{\mathbf{H}}_{\mathbf{NC}}$ (Zn) on the pathway to the native state.

The results of a number of stopped-flow kinetics studies have been reported in which actual rate enhancements have been measured as compared with our data. These rate enhancements are modest, 1.7-fold in the case of the slow phase of lysozyme refolding,[44] and 2-fold in the case of the fast phase of barstar refolding.[45] In both cases, an excess of GroEL was required to see the rate enhancement. In the particular case of barstar refolding, the rate enhancing effect could be titrated to saturation with additional GroEL, a result inconsistent with catalysis. In the particular case of lysozyme refolding, the rate enhancing effect did not lead to any obvious change in the protein-refolding pathway, a result consistent with catalysis.

However, such modest enhancements in forward rate constants have been and can be accounted for primarily in terms of simple shifts in the positions of refolding equilibria caused by the transient binding of intermediate protein refolding states to GroEL during the folding/refolding cycle (thermodynamic coupling).[15,45–47] All equilibrium constants equate *via* Haldane relationships with ratios of forward and reverse rate constants. A change in forward rate constant, not matched by an equal change in reverse rate constant (or *vice versa*), will be manifest as a change in equilibrium position. Clearly, reductions in forward rate constants observed with barnase, SNase, and here with ZnCyt c, could also be accounted for by shifts in the positions of refolding equilibria by transient binding to GroEL. Even the Iterative Annealing phenomenon where it has been observed could be neatly accounted for by extensive shifts in the positions of refolding equilibria (extensive thermodynamic coupling).[9–11] Data to date have shown that transient binding to GroEL does not appear to alter reverse protein refolding rate constants connected with protein unfolding,[47] therefore forward refolding rate constants would seem to be primarily susceptible to transient binding to GroEL and the root cause of shifts in refolding equilibria. Thus far, changes in forward rate constants (enhancements or reductions) appear to be essentially unpredictable and arbitrary. However, the extent of rate constant susceptibility should be related to a number of physical factors that may be understood in due course, including the variable natures of the unfolded substrate proteins themselves, their complexes with GroEL, the nature of the GroEL cavities, and the extrinsic refolding conditions.

Critically, since corresponding forward and reverse rate constants are apparently not being affected to equal extents by transient interactions with GroEL then there can be no catalytic effect of GroEL/GroES on protein folding/refolding, as we noted previously.[23] This whole variety of refolding rate enhancements or reductions in forward rate constants that have been observed by many research groups must surely represent little more than arbitrary substrate-dependent variations in GroEL/GroES-assisted refolding behaviour and surely cannot be the primary intended consequences of the molecular chaperone machine. Therefore, what can be the primary, core function of the GroEL/GroES molecular chaperone machine?

A unified "final theory" of GroEL/GroES-assisted protein folding/refolding has to be able to provide for a primary, core function that is also flexible enough to accommodate the evidence both for and against the Anfinsen Cage and Iterative Annealing mechanisms. We suggest that the passive kinetic partitioning mechanism proposed by ourselves and others in various guises[15,45–47] and restated here (Fig. 2), should define that core function. This mechanism provides a fundamentally thermodynamic explanation in which equilibria positions are altered through a cyclical process of binding to GroEL and timed release ("thermodynamic coupling") thereby avoiding aggregation of vulnerable folding intermediates. In our view, this process increases molecular flux through productive folding pathways and may also inadvertently generate enhancements in the forward rates of folding/refolding perhaps due to a "constructive influence on folding" by the hydrophilic character of the GroEL cavities.[20,48] Alternatively, there may be inadvertent reductions in the forward rates of folding/refolding leading *in extremis* to assisted unfolding if substrate protein-GroEL interactions are such as to encourage this to happen instead. Multiple rounds of unfolded substrate binding and release may be necessary and may take place either in the GroEL cavities or in free solution according to the size of the substrate protein involved and difficulties encountered during folding/refolding. However, we feel that such variations are best considered as arbitrary functions of either the substrate protein concerned or extrinsic refolding conditions and that the core function of GroEL/GroES-assisted folding/refolding, defined by the passive kinetic partitioning mechanism, is left unaffected.

Material and methods

General

All water used throughout was first treated with a Purite Prestige water purification system fitted with C750 carbon pre-treatment and HP700 deioniser filters. Filtered water was then further purified by the Millipore Synergy185 system to a resistance of 18.2 MΩcm. Protein purification and association experiments involving elution from a column were performed on an Amersham Pharmacia Biotech Fast Protein Liquid Chromatography (FPLC) 593 system with constant monitoring of the eluant at A_{280} absorbance. All buffers used were filtered and degassed. Sodium Dodecyl Sulfate Polyacrylamide Gel Electrophoresis (SDS PAGE) was used to visualise both the presence and purity of proteins: a full outline of the method is given in Sambrook *et al.*[49] Briefly, samples were prepared with SDS and DTT, boiled for 3 min and loaded onto Invitrogen Novex 15% Tris-Glycine Pre-cast gels in a Novex Mini-cell tank. The gels were stained with Pierce Gelcode blue stain.

GroEL and GroES purification

All experiments involving the GroE system were carried out with chaperone protein purified from *Escherichia coli* (*E. coli*) strain TG2. *E. coli* TG2 was transformed with plasmid pAM1

providing a recombinant strain, TG2/pAM1, that is able to over-express both GroEL and GroES. The construction of pAM1, its transformation into *E. coli* TG2 cells and the growth of *E. coli* TG2/pAM1 are described by Hutchinson *et al.*[22,50] *E. coli* were grown in 20 L cultures and provided as a homogenised frozen cell paste. GroEL and GroES were purified free of aromatic impurities from *E. coli* TG2/pAM1 cell paste according to procedures outlined by Tabona *et al.*[51] and Preuss *et al.*[24] The concentrated, purified solutions of both GroEL and GroES were dialysed into 50 mM Tris-HCl, pH 7.6, containing 2 mM DTT at 4 °C. Then glycerol was added up to 50% (v/v) so that samples could be stored at −20 °C without freezing. The activity of the chaperone proteins stored in these conditions was found to be undiminished over many months.[24] Concentrations of GroEL or GroES were determined by $A_{280}^{1\%}$ values calibrated by quantitative amino acid analysis for each main sample.[51] Stated GroEL and GroES concentrations always refer to the oligomer. In all cases, before experiments with ZnCyt c or cytochrome c, GroEL and GroES were dialysed into 25 mM Tris-acetate, pH 7.4, containing 2 mM β-mercaptoethanol (β-ME) (3 × 500 ml), overnight at 4 °C.

Preparation of ZnCyt c from cytochrome c

Metal free porphyrin cytochrome c (PoCyt c), was produced by removal of the Fe(II)/Fe(III) atom from the heme group of native horse-heart cytochrome c using hydrogen fluoride (HF). Owing to the hazardous nature of HF, PoCyt c production was carried out at the specialised laboratories of Dr Hoajula at the University of Manchester (Peptide Products Ltd.), based on procedures outlined by Ye *et al.*[25] Briefly, cytochrome c was dried in a desiccator *in vacuo* for 3 h to remove all traces of moisture. The dried protein was then added to anhydrous liquid HF in a Teflon flask protected from light at 0 °C. The solution was stirred for 5 min before excess HF was removed *in vacuo*; any remaining HF was blown off with dry N_2 gas. The resulting solid was dissolved in 50 mM sodium phosphate, pH 7.0, and desalted by elution through a Bio-Rad desalting column (4 × 1.5 cm) prior to lyophilisation. The dried protein was stored at −20 °C and protected from light.

ZnCyt c was prepared from PoCyt c as follows based on procedures outlined by Ye *et al.*[25] Since ZnCyt c is light sensitive, all procedures were performed in the dark and, wherever possible, at 4 °C. PoCyt c was dissolved in 25 mM Tris-acetate, pH 7.4, to a concentration of 0.5 mM, and then the solution was acidified to pH 2.5 with glacial acetic acid. An approximate 20-fold excess (w/w) of $ZnCl_2$ was added and the mixture incubated at 50 °C in a water bath for no more than 40 min. The incorporation of Zn(II) into the porphyrin was monitored by fluorescence excitation and emission spectra in an analogous manner to that described below. Following completion of the reaction, as judged by fluorescence spectroscopy, excess $ZnCl_2$ was removed by dialysis against 10% glacial acetic acid in water (made pH 3 with NaOH) for 2 h at room temperature. The mixture was then dialysed against three changes of 25 mM Tris-acetate, pH 7.4, for a total of 4 h at room temperature. Finally, the ZnCyt c solution was applied to a Pharmacia Biotech Mono S cationic exchange column (10 × 1.5 cm) previously equilibrated with 25 mM Tris-acetate, pH 7.4. The column was then washed (2 × bed volume) and the protein was eluted with 25 mM Tris-acetate, pH 7.4, containing 0.3 M NaCl. The eluant was monitored by A_{280} absorbance and peak fractions were collected manually to prevent exposure to light. SDS PAGE and UV–visible spectroscopy were used to identify peak fractions that were then concentrated using Millipore Ultrafree-15 centrifugal filters.

The concentrated solution of ZnCyt c was dialysed against three changes of 25 mM Tris-acetate, pH 7.4, to remove NaCl, after which glycerol was added to 50% glycerol (v/v) for storage at −20 °C, protected from light. The ZnCyt c concentration was determined spectroscopically using the extinction coefficient ε_{423} of 2.43×10^5 M^{-1} cm^{-1}.[52] Cytochrome c concentration was determined spectroscopically using the extinction coefficient ε_{412} of 1.06×10^5 M^{-1} cm^{-1}.[53] All spectroscopic measurements were performed in quartz cuvettes. In all cases, before experiments with GroEL and GroES, ZnCyt c and cytochrome c were dialysed into 25 mM Tris-acetate, pH 7.4, containing 2 mM β-ME (3 × 500 ml), overnight at 4 °C.

ZnCyt c denaturation in urea

Aliquots of ZnCyt c (7 μM) were equilibrated in 25 mM Tris-acetate, pH 7.4, containing 2 mM β-ME and various concentrations of urea (0–9 M) for 2 h at room temperature. Fluorescence emission spectra were recorded (Shimadzu RF-5301PC spectrofluorophotometer) for each aliquot added and corresponding background spectra, obtained from blank titrations were subtracted to give spectral data showing the increase in fluorescence intensity as a function of urea concentration.

Fluorescence binding titrations

One sample of unfolded ZnCyt c (1 μM) was prepared in 25 mM Tris-acetate, pH 7.4, containing 2 mM β-ME and 8 M urea, and left to equilibrate at room temperature for 2 h. A second sample of native ZnCyt c (1 μM) was prepared in 25 mM Tris-acetate, pH 7.4, containing 2 mM β-ME, then left to equilibrate at room temperature for 2 h as well. Aliquots of unfolded or native ZnCyt c samples were separately combined with solution aliquots containing various amounts of GroEL (0–1 μM, final concentration) in 25 mM Tris-acetate, pH 7.4, containing 2 mM β-ME. In all cases, the resulting mixtures were incubated for 30 min at 22 °C. Afterwards, fluorescence emission spectra were recorded for each mixture in turn and corresponding background spectra, obtained from blank titrations were subtracted to give spectral data showing the increase in fluorescence intensity as a function of GroEL concentration. From this data, fluorescence binding isotherms were plotted and dissociation constants determined.

Light scattering measurements

Experiments were performed in a quartz magnetic stirrer cuvette (1 cm path length). An aliquot of ZnCyt c was concentrated using Millipore Ultrafree-15 centrifugal filters (10 kDa membrane) to a concentration of 200 μM. Concentrated ZnCyt c was then equilibrated at a concentration of 150 μM in 25 mM Tris-acetate, pH 7.4, containing 2 mM β-ME and 8 M urea, for 2 h at 22 °C to unfold the protein. Unfolded, ZnCyt c was then diluted ten-fold into 25 mM Tris-acetate, pH 7.4, containing 2 mM β-ME in the presence or absence of GroEL (15 μM). Samples were placed in a cuvette and excited at 500 nm. The scattered intensity, I_{500}, was recorded as a function of time in 1 s intervals over 20 min.

Stopped flow fluorescence kinetic experiments

ZnCyt c or cytochrome c was dialysed into 25 mM Tris-acetate, pH 7.4, 2 mM β-ME (3 × 500 ml) overnight at 4 °C. The protein (20 μM) was unfolded by incubation in 25 mM Tris-acetate, pH 7.4, containing 2 mM β-ME and 8 M urea for 2 h at room temperature in order to unfold. Unfolded ZnCyt c or cytochrome c was refolded by rapid ten-fold dilution into either 25 mM Tris-acetate, pH 7.4, containing 2 mM β-ME alone (2 μM, final ZnCyt c or cytochrome c concentration), or else ZnCyt c alone was diluted ten-fold into the same buffer containing in addition either; 0.05–4 μM GroEL: 1.2–4.8 μM bovine serum albumin (BSA): 2 μM GroEL-mMDH (see below): 0.05–4 μM GroEL, 1 mM ADP, 10 mM $MgCl_2$ and 10 mM KCl: 0.05–4 μM GroEL, 1 mM ATP, 10 mM $MgCl_2$ and 10 mM KCl: or 0.05–4 μM GroEL, 0.05–10 μM GroES, 1 mM ATP, 10 mM $MgCl_2$ and 10 mM KCl.

Measurements were carried out on a BioLogic SFM-3 Stopped Flow in conjunction with an MPS-52 microprocessor. Fluorescence measurements were made using an ALX-220 arc lamp. For intrinsic tryptophan fluorescence, the excitation wavelength was set at 280 nm and the intrinsic fluorescence monitored above 320 nm with a cut-off filter. For intrinsic Zn(II)porphyrin fluorescence, the excitation wavelength was 409 nm and the intrinsic fluorescence was monitored above 455 nm. Temperature was maintained constant at 22 °C throughout by means of a water bath. Between experiments, in order to ensure expulsion of aged samples, the cuvette was first cleared with three shots of unrecorded sample. Data points for each recorded shot were collected every 500 μs for the first 500 ms, every 2 ms between 500 ms and 2.3 s and every 20 ms from 2.3 s to 30 s. Each pure ZnCyt c refolding experiment was repeated five times in succession and data was averaged using the Biokine software. For experiments involving different concentrations of GroEL, each ZnCyt c refolding experiment concentration was performed in triplicate, interpreted separately and errors calculated by standard deviation. Data were output into the BioLogic Biokine software as plots of voltage against time. Kinetic rates were then determined by fitting the curve to eqn (2):

$$V = at + b \sum c_i \cdot \exp(-k_i t) \quad (2)$$

where V is voltage (amplitude), a, b, and c_i are constants, t is time and k_i the i-th rate constant (where $i = 1$–3).

Preparation of GroEL–mMDH complex

mMDH (100 μM) was incubated in 25 mM Tris-acetate, pH 7.4, containing 2 mM β-ME and 8 M urea for 2 h at room temperature, in order to unfold. Thereafter unfolded mMDH was diluted ten-fold into 25 mM Tris-acetate, pH 7.4, containing 2 mM β-ME and GroEL (5 μM). The mixture was incubated for 30 min at room temperature. The mixture was then applied to a Sephadex S-300 column (0.9 × 15 cm) and eluted with 25 mM Tris-acetate, pH 7.4, containing 2 mM β-ME at a flow rate of 1 ml min^{-1}. The eluant was collected in fractions (1 ml) on ice. SDS PAGE was used to identify fractions containing GroEL–mMDH complex which were then combined and concentrated using Millipore Ultrafree-15 centrifugal filters (100 kDa membrane). The concentration of free GroEL was assumed to be negligible.

Conclusion

In conclusion, we propose that the passive kinetic partitioning mechanism should be adopted as the cleanest and simplest way to characterise the core function of the GroEL/GroES molecular chaperone, a primary, basic function that gives a clear cut reason for why the GroEL/GroES molecular chaperone is known as a "folding machine for many but a master of none".[21]

Abbreviations

GroEL, Hsp60 class oligomeric molecular chaperone (chaperonin); GroES, Hsp10 class oligomeric molecular co-chaperone (co-chaperonin); ZnCyt c, zinc-cytochrome c; PoCyt c, metal free porphyrin cytochrome c; mMDH, mitochondrial malate dehydrogenase; DHFR, dihydrofolate reductase; CS, citrate synthase; SNase, staphylococcal nuclease; α-LA, α-lactalbumin; β-ME, β-mercaptoethanol.

Acknowledgements

Imperial College Genetic Therapies Centre is grateful to the Mitsubishi Chemical Corporation and IC-Vec Ltd for financial support.

References

1 F. U. Hartl and M. Hayer-Hartl, *Science*, 2002, **295**, 1852–1858.
2 H. S. Chan and K. A. Dill, *Proteins: Struct., Funct., Genet.*, 1996, **24**, 345–351.
3 R. J. Ellis, *Curr. Biol.*, 2001, **11**, R1038–1040.
4 R. J. Ellis, *Curr. Biol.*, 2003, **13**, R881–883.
5 T. K. Chaudhuri, G. W. Farr, W. A. Fenton, S. Rospert and A. L. Horwich, *Cell*, 2001, **107**, 235–246.
6 G. W. Farr, W. A. Fenton, T. K. Chaudhuri, D. K. Clare, H. R. Saibil and A. L. Horwich, *EMBO J.*, 2003, **22**, 3220–3230.
7 M. J. Todd, P. V. Viitanen and G. H. Lorimer, *Science*, 1994, **265**, 659–666.
8 J. S. Weissman, Y. Kashi, W. A. Fenton and A. L. Horwich, *Cell*, 1994, **78**, 693–702.
9 N. A. Ranson, N. J. Dunster, S. G. Burston and A. R. Clarke, *J. Mol. Biol.*, 1995, **250**, 581–586.
10 M. Shtilerman, G. H. Lorimer and S. W. Englander, *Science*, 1999, **284**, 822–825.
11 M. J. Todd, G. H. Lorimer and D. Thirumalai, *Proc. Natl. Acad. Sci. U. S. A.*, 1996, **93**, 4030–4035.
12 J. Chen, S. Walter, A. L. Horwich and D. L. Smith, *Nat. Struct. Biol.*, 2001, **8**, 721–728.
13 E. S. Park, W. A. Fenton and A. L. Horwich, *FEBS Lett.*, 2005, **579**, 1183–1186.
14 M. Preuss and A. D. Miller, *FEBS Letters*, 1999, **461**, 131–135.
15 C. M. Smith, R. J. Kohler, E. Barho, T. S. H. El-Thaher, M. Preuss and A. D. Miller, *J. Chem. Soc., Perkin Trans. 2*, 1999, 1537–1546.
16 G. S. Jackson, R. A. Staniforth, D. J. Halsall, T. Atkinson, J. J. Holbrook, A. R. Clarke and S. G. Burston, *Biochemistry*, 1993, **32**, 2554–2563.
17 J. Buchner, M. Schmidt, M. Fuchs, R. Jaenicke, R. Rudolph, F. X. Schmid and T. Kiefhaber, *Biochemistry*, 1991, **30**, 1586–1591.
18 R. J. Kohler, M. Preuss and A. D. Miller, *Biotechnol. Prog.*, 2000, **16**, 671–675.
19 R. J. Kohler, M. Preuss, H. Jones and A. D. Miller, Protein affinity purification and analysis technologies, *Gene cloning and expression technologies*, ed. M. P. Weiner and Q. Lu, Eaton Publishing, Westborough, MA, 2002, pp. 439–445.
20 J. D. Wang, C. Herman, K. A. Tipton, C. A. Gross and J. S. Weissman, *Cell*, 2002, **111**, 1027–1039.
21 A. Erbse, D. A. Dougan and B. Bukau, *Nat. Struct. Biol.*, 2003, **10**, 84–86.

22 J. P. Hutchinson, T. S. H. El-Thaher and A. D. Miller, *Biochem. J.*, 1994, **302**, 405–410.
23 A. D. Miller, K. Maghlaoui, G. Albanese, D. A. Kleinjan and C. Smith, *Biochem. J.*, 1993, **291**, 139–144.
24 M. Preuss, J. P. Hutchinson and A. D. Miller, *Biochemistry*, 1999, **38**, 10272–10286.
25 S. Ye, C. Shen, T. M. Cotton and N. M. Kostic, *J. Inorg. Biochem.*, 1997, **65**, 219–226.
26 H. Anni, J. M. Vanderkooi and L. Mayne, *Biochemistry*, 1995, **34**, 5744–5753.
27 J. M. Vanderkooi and M. Erecinska, *Eur. J. Biochem.*, 1975, **60**, 199–207.
28 V. Logovinsky, A. D. Kaposi and J. M. Vanderkooi, *Biochim. Biophys. Acta*, 1993, **1161**, 149–160.
29 A. C. Clark and C. Frieden, *J. Mol. Biol.*, 1997, **268**, 512–525.
30 M. C. Shastry, J. M. Sauder and H. Roder, *Acc. Chem. Res.*, 1998, **31**, 717–725.
31 H. S. Rye, S. G. Burston, W. A. Fenton, J. M. Beechem, Z. Xu, P. B. Sigler and A. L. Horwich, *Nature*, 1997, **388**, 792–798.
32 W. Colón, G. A. Elöve, L. P. Wakem, F. Sherman and H. Roder, *Biochemistry*, 1996, **35**, 5538–5549.
33 W. Colón, L. P. Wakem, F. Sherman and H. Roder, *Biochemistry*, 1997, **36**, 12535–12541.
34 H. Roder, G. A. Elove and S. W. Englander, *Nature*, 1988, **335**, 700–704.
35 D. N. Brems and E. Stellwagen, *J. Biol. Chem.*, 1983, **258**, 3655–3660.
36 H. Yang and D. L. Smith, *Biochemistry*, 1997, **36**, 14992–14999.
37 F. J. Corrales and A. R. Fersht, *Proc. Natl. Acad. Sci. U. S. A.*, 1995, **92**, 5326–5330.
38 T. E. Gray and A. R. Fersht, *J. Mol. Biol.*, 1993, **232**, 1197–1207.
39 G. P. Tsurupa, T. Ikura, T. Makio and K. Kuwajima, *J. Mol. Biol.*, 1998, **277**, 733–745.
40 K. Kuwajima, *FASEB J.*, 1996, **10**, 102–109.
41 K. Katsumata, A. Okazaki and K. Kuwajima, *J. Mol. Biol.*, 1996, **258**, 827–838.
42 T. Makio, M. Arai and K. Kuwajima, *J. Mol. Biol.*, 1999, **293**, 125–137.
43 M. Preuss and A. D. Miller, *FEBS Lett.*, 2000, **466**, 75–79.
44 J. E. Coyle, F. L. Texter, A. E. Ashcroft, D. Masselos, C. V. Robinson and S. E. Radford, *Nat. Struct. Biol.*, 1999, **6**, 683–690.
45 N. Bhutani and J. B. Udgaonkar, *J. Mol. Biol.*, 2000, **297**, 1037–1044.
46 Y. Fridmann, S. Ulitzur and A. Horovitz, *J. Biol. Chem.*, 2000, **275**, 37951–37956.
47 S. Walter, G. H. Lorimer and F. X. Schmid, *Proc. Natl. Acad. Sci. U. S. A.*, 1996, **93**, 9425–9430.
48 A. Brinker, G. Pfeifer, M. J. Kerner, D. J. Naylor, F. U. Hartl and M. Hayer-Hartl, *Cell*, 2001, **107**, 223–233.
49 J. Sambrook and D. Russell, *Commonly used techniques in molecular cloning*, Cold Spring Harbor Laboratory Press, New York, 2001.
50 J. P. Hutchinson, T. C. Oldham, T. S. H. El-Thaher and A. D. Miller, *J. Chem. Soc., Perkin Trans. 2*, 1997, 279–288.
51 P. Tabona, K. Reddi, S. Khan, S. P. Nair, S. V. Crean, S. Meghji, M. Wilson, M. Preuss, A. D. Miller, S. Poole, S. Carne and B. Henderson, *J. Immunol.*, 1998, **161**, 1414–1421.
52 M. M. Crnogorac and N. M. Kostic, *Inorg. Chem.*, 2000, **39**, 5028–5035.
53 E. Margoliash and A. Schejter, *Adv. Protein Chem.*, 1966, **21**, 113–286.
54 Z. H. Xu and P. B. Sigler, *J. Struct. Biol.*, 1998, **124**, 129–141.
55 G. W. Bushnell, G. V. Louie and G. D. Brayer, *J. Mol. Biol.*, 1990, **214**, 585–595.